Fitzgerald *et al. Microbiome* (2025) 13:201
https://doi.org/10.1186/s40168-025-02220-9

Microbiome

RESEARCH

Open Access

Members of *Lachnospiraceae* produce valerate and caproate in response to short-chain fatty acids

Bradley G. Fitzgerald[1], Manitabhai Govind[1], Isaac J. Firth[1], Loudon Herold[1], Julia Froment[1], Sarah J. Vancuren[1], Emma Allen-Vercoe[1], Matthew S. Kimber[1] and Matthew T. Sorbara[1*]

Abstract

Background The human gut microbiota ferments carbohydrates to produce metabolites that mediate beneficial community functions. While the production of the short-chain fatty acids (SCFAs) acetate, propionate, and butyrate is well characterized, how valerate and caproate are produced has remained enigmatic.

Results Here, we characterize the production of valerate and caproate by the gut microbiota. In a continuous culture model of a defined gut bacterial community, we observed that valerate took longer to reach physiological levels than acetate, propionate, or butyrate and correlated with *Lachnospiraceae*. This led us to test valerate and caproate production by members of *Lachnospiraceae*. While tested *Lachnospiraceae* isolates produced low levels of valerate and caproate at baseline, physiological concentrations of SCFAs activated valerate and caproate production in a species-specific manner. Furthermore, providing isotopically labelled SCFAs revealed that isolates of *Anaerostipes hadrus* and *Coprococcus comes*, which are members of *Lachnospiraceae*, directly incorporate exogenous acetate, propionate, and butyrate into valerate and caproate in a manner consistent with the reverse β-oxidation pathway. Therefore, we examined this pathway in *Lachnospiraceae* and found that *Lachnospiraceae* spp. encode different copy numbers and variants of the enzyme acetyl-CoA acetyltransferase (ThlA). ThlA performs the first step in reverse β-oxidation by condensing acyl-CoA molecules. We demonstrate that tested *Lachnospiraceae* ThlA protein variants consume propionyl-CoA and acetyl-CoA substrates consistent with valerate production. *Coprococcus comes*, the only tested species to produce caproate, encodes a second ThlA protein with increased activity on butyryl-CoA. In human fecal samples, multiple genera of *Lachnospiraceae* correlate with butyrate, while *Coprococcus* also correlates with caproate levels.

Conclusions These findings reveal a role of certain members of the *Lachnospiraceae* as prominent producers of valerate and caproate within human microbiomes through the reverse β-oxidation pathway.

Introduction

In the anoxic environment of the colon, the microbiota ferments carbohydrates, including dietary polysaccharides that are otherwise inaccessible to the host. This metabolic activity leads to the production of short-chain fatty acids (SCFAs), which include acetate, propionate, and butyrate [1, 2]. Production of acetate, propionate, and butyrate has been well characterized and they accumulate to 12.8–103.4 mmol/kg (37.4 median), 4.5–27.8 mmol/kg (12.5 median), and 4.0–53.0 mmol/kg (12.4 median) in human fecal samples, respectively [3, 4]. Indeed, the ability to produce acetate is widely distributed across gut taxa, and multiple pathways for butyrate and propionate have been characterized [5–8]. However, these are not the only fermentation metabolites produced, as valerate and caproate are also produced by the microbiota and range in human fecal samples from 0.6 to 3.8 mmol/kg

*Correspondence:
Matthew T. Sorbara
msorbara@uoguelph.ca
[1] Department of Molecular and Cellular Biology, University of Guelph, Guelph, ON, Canada

(2.4 median) and 0 to 3.6 mmol/kg (0.5 median), respectively [4]. Valerate and caproate have variably been categorized as SCFAs or medium-chain fatty acids [9, 10]. Notably, in comparison to SCFAs, less is known about valerate and caproate production in the gut.

SCFAs contribute to colonization resistance, provide an energy source for colonocytes, and modulate the immune system [1, 11–13]. Interestingly, recent studies have also uncovered important roles for valerate and caproate. For example, valerate inhibits *Clostridiodes difficile* at concentrations between 2 and 20 mM, and thus contributes to colonization resistance [14]. At the cellular level, valerate acts as a histone deacetylase (HDAC) inhibitor in $CD8^+$ T cells, altering gene expression at concentrations between 250 μM and 2.5 mM [15]. Furthermore, exposure to 300 μM to 2 mM of valerate reduces IL-17A production in $CD4^+$ T cells, proinflammatory cytokine production in macrophages, and regulates intestinal barrier function in colonic epithelial cells [16–18]. In mice, valerate levels decrease during intestinal inflammation in a dextran sodium sulfate (DSS) model, and, in this model, valerate administration by intraperitoneal injection ameliorates inflammation [18]. In agreement, recent meta-analyses indicate that decreases in valerate are more consistent across cohorts compared to the decrease of SCFAs in patients with inflammatory bowel disease (IBD) [19, 20]. Further, it has been reported that caproate is decreased in IBD patients [21]. Given the accumulating evidence that valerate and caproate are functional, health-associated metabolites, identifying which microbes produce them and how production is regulated represents an important question.

While relatively little is known about valerate and caproate production by the gut microbiota compared to SCFAs, there are known metabolic pathways that yield these metabolites. First, valerate and caproate can be produced through fermentation of amino acids using amidase enzymes [22–25], and in agreement, supplementation of various amino acids can increase levels in a complex community [24]. Alternatively, *Megasphaera* spp., which are commonly used in industrial settings and can also be gut residents, produce valerate and caproate through the reverse β-oxidation pathway [10, 26]. This pathway is dependent on an acetyl-CoA acetyltransferase enzyme (EC 2.3.1.9, denoted here as ThlA), which, in *Megasphaera* spp., condenses acyl-CoA molecules of varying lengths to yield butyrate, valerate, caproate, and longer fatty acids. However, whether amino acid metabolism or the presence of *Megasphaera* accounts for valerate and caproate production in most human microbiomes remains unclear.

Lachnospiraceae are gram-positive anaerobes that are prevalent and abundant in the human gut microbiota [27]. Collectively, they are important contributors to SCFA production [28]. Some species, such as *Blautia* spp., are acetogenic and produce high levels of acetate [6]. Others, such as *Anaerostipes hadrus* and *Coprococcus comes,* produce butyrate using a reverse β-oxidation pathway and either butyrate kinase or butyrate transferase to convert butyryl-CoA to butyrate [27, 29]. Although there are exceptions [30], *Lachnospiraceae* are often health associated, and their SCFA production ability enables them to contribute to colonization resistance and other beneficial microbiome functions [11, 31]. However, whether *Lachnospiraceae* contribute to valerate or caproate production is unknown.

Here, we examined valerate and caproate production by the gut microbiota. Unexpectedly, we found that valerate accumulation to physiological levels is slower than SCFAs in a continuous culture model of the colonic microbiome and correlates with *Lachnospiraceae*. This led us to test production by *Lachnospiraceae* isolates. We found that, while production of valerate or caproate is low under baseline conditions, supplementation with exogenous SCFAs activates significant valerate and/or caproate production in a species-dependent manner by butyrate-producing *Lachnospiraceae*. All tested butyrate-producing *Lachnospiraceae* directly incorporate exogenous propionate into valerate, while only *C. comes* incorporates butyrate into caproate. Unlike isolates of the other tested species, isolates of *C. comes* encode a second ThlA enzyme with a larger active site tunnel, which shows greater consumption of butyryl-CoA. This indicates that variations in ThlA enzymes can impact valerate and caproate production. Finally, we found that, while *Megasphaera* is present in the gut microbiota of some individuals [32, 33], valerate- and caproate-producing *Lachnospiraceae* genera are more prevalent. Furthermore, both *Coprococcus* and *Megasphaera* significantly correlate with caproate in stool samples. Overall, this reveals that a select group of *Lachnospiraceae* produce physiological levels of valerate and caproate in high SCFA environments like the colon.

Materials and methods

In vitro continuous culture model

Infors Multiflors 2 bioreactor vessels (Infors HT) were used to culture a defined community of bacterial strains in a continuous culture system, as previously described [34]. In these experiments, biological replicates were defined as independent vessels. Healthy human donor-derived strains included in the community are listed in Table S1 [35]. The vessels were fed a mucin-based media designed to mimic the colonic environment, maintained at pH 6 with HCl or NaOH, and maintained under anaerobic conditions with nitrogen sparging. Media

composition is as described by [36]. Vessels were operated in batch mode for the first 24 h before switching to continuous culture operation with a retention time of 24 h. Daily samples were collected and centrifuged at 13,000×*g* for 3 min. Supernatant was collected for gas chromatography mass spectrometry (GC–MS) analysis, and DNA was extracted from the pellet using the QIAamp PowerFecal Pro DNA Kit (Qiagen, USA), with the following modifications: after samples were subjected to bead-beating for 20 min, they were incubated in a 95 °C water bath for 10 min and sonicated for 5 min, after which Proteinase K (Thermo Fisher) was added to a final concentration of 19.5 mg/mL with incubation at 70 °C for 10 min. The protocol then proceeded according to the manufacturer's directions. 16S rRNA 300 bp sequencing of V3–V4 amplicon was performed by the University of Guelph Genomics Facility by Illumina MiSeq. Sequencing reads were then filtered/trimmed, grouped into amplicon sequence variations, and assigned taxonomy using the DADA2 package [37]. PCoA graphs were generated using Bray–Curtis dissimilarity.

Bacterial Strains and Growth

Strains

All *Blautia* spp., *Anaerostipes hadrus, Coprococcus comes,* and *Eubacterium rectale* strains were previously isolated from healthy human donors as described in [27]. *Roseburia* spp. strains and strains included in the donor-derived defined community were previously isolated and reported in [35]. A complete list of strains is provided in Table S1. Species included in the 6-strain consortium were *A. hadrus, C. comes, Blautia luti, Clostridium innocuum, Clostridium symbiosum*, and *Dorea longicatena*, with or without *Anaerotignum lactatifermentans* (see Table S1).

Growth

All bacterial strains were grown in an anaerobic chamber (Coy Laboratory Products), supplied with a gas mix of 90% N_2, 5% CO_2, and 5% H_2. The strains were streaked on pre-reduced brain heart infusion agar plates, supplemented with 0.5% yeast extract and 0.1% cysteine (BHIS-agar). Isolated colonies were suspended in pre-reduced PBS, which was used to inoculate BHIS broth at a 1:100 dilution. Unless otherwise stated, *Lachnospiraceae* strains in broth and on plates were grown at 37 °C for 16 h. For broth cultures, 200 µL were collected for OD_{600} to measure growth, and a 1-mL aliquot was collected and centrifuged at 13,000×*g* for 3 min. The supernatant was stored at − 80 °C until GC–MS analysis. For in vitro experiments, at least three independent biological replicates were performed. Biological replicates were defined as independent assays performed on different days with bacteria inoculated from different streak plates made from frozen glycerol stocks.

SCFA assay broth

BHIS supplemented with SCFAs was prepared by adding acetic acid, propionic acid, or butyric acid at concentrations of 30 mM, 10 mM, and 10 mM, respectively, to autoclaved BHIS. For individual SCFA assays, propionic acid or butyric acid was added at 10 mM. pH in the SCFA supplemented BHIS was corrected to 7 using NaOH. For isotopically-labelled SCFA experiments, $2C^{13}$ acetate, $3C^{13}$ propionate, and $4C^{13}$ butyrate were used (Sigma-Aldrich). Supplemented broths were filter sterilized and reduced in the anaerobic chamber overnight.

Intracellular acyl-CoA analysis

Bacterial strains were grown in BHIS at 37 °C with or without SCFAs, as above, for 4 h until mid-exponential phase. The strains were then chemically lysed using a bacterial protein lysis buffer kit (Biobasic, USA), as per the manufacturer's instructions. The lysate was stored at − 80 °C for GC–MS analysis.

Inositol assay broth

BHIS broth without dextrose (Alpha Bioscience, USA), supplemented with 0.5% yeast extract and 0.1% cysteine, was diluted 1:1 with water containing 5% w/v of the respective sugar. The broth was syringe filtered and reduced in the anaerobic chamber overnight.

Metabolomics

Fatty acids and amino acids

Targeted metabolomics analysis was performed on collected bacterial culture supernatant samples as previously described in [38]. Briefly, supernatant samples were suspended in ice-cold methanol (4:1) containing internal standards of D3-acetate and D7-butyrate. Following thorough mixing, the samples were centrifuged at 13,000×*g* at 4 °C for 18 min. 100 µL of the supernatant was transferred to a 2-mL glass vial and 100 µL of borate buffer (pH 10), 400 µL of acetonitrile with 150 mM pentafluorobenzyl bromide (PFBBr–Sigma-Aldrich) and 600 µL of hexane were added. The samples were incubated in a thermomixer at 65 °C for 1 h with shaking at 1500 rpm. Following incubation, 400 µL of hexane was extracted from the organic layer and 1 µL was injected into an Agilent GC–MS (5977B) with a 10:1 split. The samples were analyzed in negative chemical ionization mode using methane as the reagent gas and helium as the carrier gas. Peaks were identified using Mass Hunter Quantitative and normalized to the internal standards. Concentration values were calculated using a standard curve for acetate (CAS: 71–50-1), propionate (CAS: 72–03-7),

butyrate (CAS: 107–92-6), valerate (CAS: 10,023–74-2) and caproate (CAS: 151–33-7). Fold changes for isobutyrate (CAS: 5711–69-3), isovalerate (CAS: 503–74-2), valine (CAS: 72–18-4), leucine (CAS: 61–90-5), isoleucine (CAS: 73–32-5), and glutamate (CAS: 11,070–68-1) were calculated by normalizing peak areas to D3-acetate.

Acyl-CoA

Acyl-CoA derivatives (Acetyl-CoA, Propionyl-CoA and Butyryl-CoA) were detected using glycine aminolysis and PFBBr derivatization as previously described [39]. Briefly, 0.5 M glycine in ethanol was added to the sample at a 1:2 ratio. The pH was corrected to 10 using NaOH, and the samples were incubated at 70 °C for 4 h. Following incubation, the pH was corrected to 1 using HCl, and the sample was suspended in methylene chloride (1:100) to extract the *N*-acylglycines. The samples were dried down in a speedvac, and then *N*-acylglycines were derivatized by adding 30 µL of acetonitrile, 10 µl of 35% PFBBr in acetonitrile, and 10 µL of diisopropylethylamine. The reactants were incubated at 40 °C for 30 min, and then the solvent was evaporated using a speedvac. The derivatized *N*-acylglycines were suspended in 200 µL of methylene chloride and thoroughly mixed. 80 µL was transferred to a glass Agilent vial, and 1 µL was injected into the GC–MS. The samples were analyzed in negative chemical ionization mode using methane as the reagent gas and helium as the carrier gas. The peaks were identified using Mass Hunter Quantitative and normalized to the glycine.

Acetyl-CoA Acetyltransferase Analysis

thlA analysis

Bacterial whole genome sequences from previously published gut microbe biobanks [27, 40–42] (accession numbers: PRJNA596270, PRJNA544527, PRJNA482748, and PRJNA412637) were annotated through Prokka [43]. *Roseburia* spp. DNA was extracted, as above, and genomes were sequenced by Plasmidsaurus Inc using Oxford Nanopore (ONT) long reads. Gene copy number plots and operons were generated in R Studio. Protein and nucleotide sequences were aligned using MUSCLE v5 [44]. A thlA maximum likelihood tree was generated using RAXML [45] and the 16S rRNA dendrogram tree with *thlA* gene copy numbers was generated using hierarchical clustering.

Structure analysis

Predicted ThlA protein structures were generated using Alphafold 3 [46]. Acetobutyryl-CoA binding was modeled using Chai-1 [47]. Structures were visualized in PyMol.

Human Microbiome Project

16S rRNA abundance data was downloaded from the iHMP data [32, 33] portal along with the associated metadata. The paired metabolomics were downloaded from the NIH Common Fund's Metabolomics Data Repository and Coordinating Center (Project ID: PR000639).

ThlA Protein Assay

pET29-b(-) plasmids with the individual thlA genes containing 6xHis tags and kanamycin resistance were ordered from Twist Bioscience (South San Francisco, USA). The plasmids were then transformed into chemically competent *E. coli* (DH5α) using the heat shock method and plated with LB media containing 50 mg/mL kanamycin. Single isolated colonies were used to inoculate overnight cultures. The plasmids were then extracted using a miniprep kit (Thermo Scientific), as per the manufacturer's instructions and sequenced through Sanger sequencing by the University of Guelph Genomics Facility. The plasmids were transformed into chemically competent *E. coli* (BL21 DE3), made in-house and grown in 1 L cultures at 37 °C until an OD_{600} value of 0.6–0.8 was obtained. Next, 1 mM IPTG (dioxane-free) was utilized to induce plasmid expression at 16 °C for 20 h, and the cells were harvested by centrifuging at 5000×*g* for 30 min. The pellet was then resuspended in an extraction buffer (50 mM tris pH 8.0, 500 mM NaCl, 500 mM imidazole, 2 mM DTT) together with 1 mM phenylmethylsulfonyl fluoride and lysed using a sonicator. The protein lysates were obtained by centrifuging at 50,000×*g* for 30 min. Immobilized metal affinity chromatography (IMAC) with a 1-mL HisTrap HP column attached to a peristaltic pump was used for protein purification from the lysate. The proteins were eluted using an increasing gradient of imidazole (20–500 mM). SDS-PAGE and Coomassie staining were used to confirm purification. The proteins were then desalted into a minimal buffer (50 mM tris pH 8.0, 150 mM NaCl, 500 mM, 2 mM DTT) using gravity columns and concentrated using an Amicon® Ultra-15 Centrifugal Filter Unit 10 kDa. Finally, the concentrated proteins were quantified using a NanoDrop2000 spectrophotometer and frozen at − 80 °C.

The ability of these ThlA proteins to catalyze reactions with the acyl-CoA derivatives (acetyl-CoA, propionyl-CoA and butyryl-CoA) was determined using previously described methods in [48]. Briefly, ThlA (100 ng/ml) variants were added to 50 mM Tris–HCl (pH 7.4), 0.2 mM NADH, acyl-CoA derivatives (acetyl-CoA 5 mM when independent or 0.5 mM with other acyl-CoAs, propionyl-CoA 5 mM and butyryl-CoA 10 mM) and excess 17-β-hydroxysteroid dehydrogenase (Hsd4a). The mixture was incubated at 37 °C for 2 h and then stored at − 80 °C until GC–MS analysis.

Statistical Analysis

Statistics were performed using R Studio. One-way ANOVA calculations were performed with post-hoc Tukey test. In the ThlA activity assay, the variance across enzymes was not equal and therefore, a pairwise t-test with Bonferroni correction was utilized that confirmed the results of a one-way ANOVA with post-hoc Tukey test. P values < 0.05 were considered significant. Spearman correlations were used to assess the continuous culture model and the Human Microbiome Project data.

Results

Distinct accumulation kinetics of SCFA and valerate in a microbial community

Given the importance of valerate in host-microbe and microbe-microbe interactions, we sought to investigate how the microbiota produces valerate. We established a 126-strain gut microbe community in a continuous culture bioreactor fed a complex, mucin-containing media representing nutrients available in the colon (Table S1) [35]. Using this system, we tracked daily changes in community composition and metabolite production (Fig. 1A). By day 11, the concentrations and relative ratios of SCFAs and valerate were within physiological ranges with higher concentrations of acetate, propionate, and butyrate compared to valerate (Fig. 1B) [4, 49–51]. Caproate did not accumulate in this system (*data not shown*). Next, we examined daily samples to determine the kinetics of SCFA and valerate accumulation. This revealed that acetate was the first SCFA to accumulate to physiological concentrations and reached > 40 mM on day two before plateauing or declining (Fig. 1C and Fig. S1A). Initially, propionate and butyrate accumulated rapidly and reached > 10 mM on day 3 (Fig. 1C and Fig. S1A). After this initial phase, the accumulation of propionate and butyrate slowed or plateaued (Fig. 1C and Fig. S1A). Interestingly, valerate showed the slowest kinetics of accumulation and reached > 1 mM at day nine and was continuing to increase at day eleven (Fig. 1C and Fig. S1A). At days 2 and 3, when SCFAs were already at high levels, the valerate concentration was below 0.5 mM. We noted that, while the overall pattern of SCFA accumulation was consistent, individual reactors showed variation in SCFA concentrations over the run; however, all had slower valerate accumulation compared to the SCFAs (Fig. S1A).

Next, we measured changes in community composition. As expected for a colonic microbiota, on day eleven, the *Bacillota* and *Bacteroidota* phyla were the most abundant and represent > 90% of the community, alongside lower levels of *Actinomycetota* or *Pseudomonadota* (Fig. 1D). *Lachnospiraceae* and *Bacteroidaceae* were the most abundant families (Fig. 1E). Overall, replicate communities showed consistent progression in composition over time (Fig. S1BC). However, in line with variations in SCFA concentrations (Fig. S1A), we noted modest variations in community progression in individual reactors. Replicates one and two had increased *Bifidobacteriaceae* at early timepoints and lower *Bacteroidaceae* with higher *Lachnospiracea*e at later timepoints compared to replicates three and four (Fig. S1AC).

Next, we used the dynamic nature of these communities and correlated daily relative abundances of microbial families with SCFA and valerate levels. This revealed that *Lachnospiraceae* were the family which most strongly correlated with valerate (Fig. 1FG). However, *Lachnospiraceae* also positively correlated with propionate and butyrate (Fig. 1F and Fig. S1D). Furthermore, we noted that *Bacteroidaceae* also correlated with the SCFAs and valerate (Fig. 1F). Overall, none of the abundant families correlated exclusively with valerate (Fig. 1F).

Exogenous SCFAs altered valerate and caproate production

Since the accumulation of valerate to physiological levels was slower than SCFAs, we asked whether extracellular SCFAs regulate valerate production. We focused our initial analysis on *Lachnospiraceae* since they had the strongest correlation with valerate. We profiled SCFA, valerate, and caproate production by 9 *Lachnospiraceae* isolates in the presence and absence of exogenous SCFAs. Under baseline conditions, isolates of the acetogenic *Blautia* genus produced acetate but not propionate, butyrate, or valerate (Fig. 2A–C and Fig. S2A). As expected, *A. hadrus* and *C. comes* isolates produced 5–10 mM of butyrate (Fig. 2B). Furthermore, *A. hadrus* isolates reduced acetate present in the media by 1.3 mM on average, while isolates of *C. comes* increased acetate concentrations by 8.3 mM (Fig. 2A). Interestingly, none of the tested *Lachnospiraceae* isolates released valerate under these growth conditions. However, valerate production significantly increased when the butyrate-producing *Lachnospiraceae* isolates were grown with a physiological mix of exogenous SCFAs (Fig. 2C). In contrast, *Blautia* isolates did not exhibit SCFA-regulated valerate production. Under these conditions, the tested *Lachnospiraceae* strains did not produce isobutyrate or isovalerate and did not deplete valine, leucine, isoleucine, or glutamate that have been previously linked to valerate, isobutyrate, and isovalerate production through amino acid fermentation (Fig. S2B–D) [24, 25]. Interestingly, we observed inter-species variability, with isolates of *C. comes* producing an average of 427 μM of valerate compared to 108 μM in *A. hadrus* cultures (Fig. 2C). Next, we measured caproate production and found that only *C. comes*

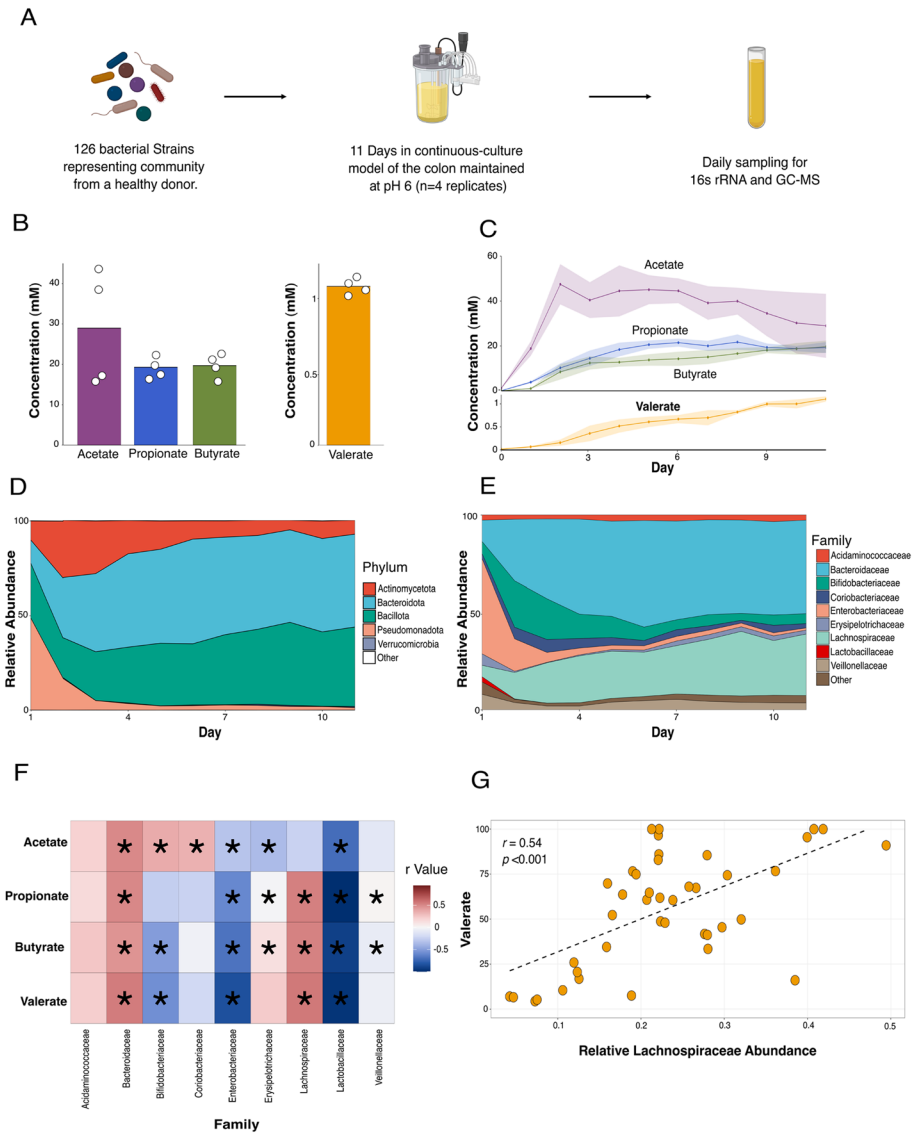

Fig. 1 SCFAs and valerate accumulate in a model of the gut microbiota and correlate with *Lachnospiraceae*. **A** Schematic of a continuous culture colon model used to grow a 126 bacterial strain community for 11 days with daily sampling for GC–MS and 16S rRNA analysis. **B** At day 11, SCFA and valerate concentrations reach physiological levels ($n = 4$ continuous culture runs). **C** Accumulation kinetics of valerate is slower compared to the accumulation of acetate, propionate, and butyrate (SCFAs) (mean concentration ± standard deviation). **D**, **E** Mean community composition at phylum (**D**) and family (**E**) levels rapidly stabilizes after day 3 ($n = 4$ continuous culture runs). **F** Spearman correlations between the most abundant families and SCFA/valerate accumulation. **G** Spearman correlation of relative *Lachnospiraceae* abundance and valerate accumulation. * indicates $p < 0.05$

produced caproate, which increased with SCFA supplementation from 18 to 25 µM (Fig. 2D). Since SCFAs can alter microbial growth [52], we measured *Lachnospiraceae* growth under these SCFA-supplemented conditions. Interestingly, exogenous SCFAs increased the growth of most valerate-producing *C. comes* and *A. hadrus* strains, whereas no difference was observed for two *Blautia* strains or one strain of *A.hadrus* (Fig. S2E). Together, this demonstrates that exogenous SCFAs activate valerate and caproate production in a species-dependent manner.

Next, we determined if valerate and caproate production was triggered by specific SCFAs, and expanded the tested species to include strains of butyrate-producing *Eubacterium rectale* (also known as *Agathobacter rectalis*) and *Roseburia* spp. Exogenous propionate, but not butyrate, activated valerate production by all tested butyrate-producing *Lachnospiraceae* isolates, and

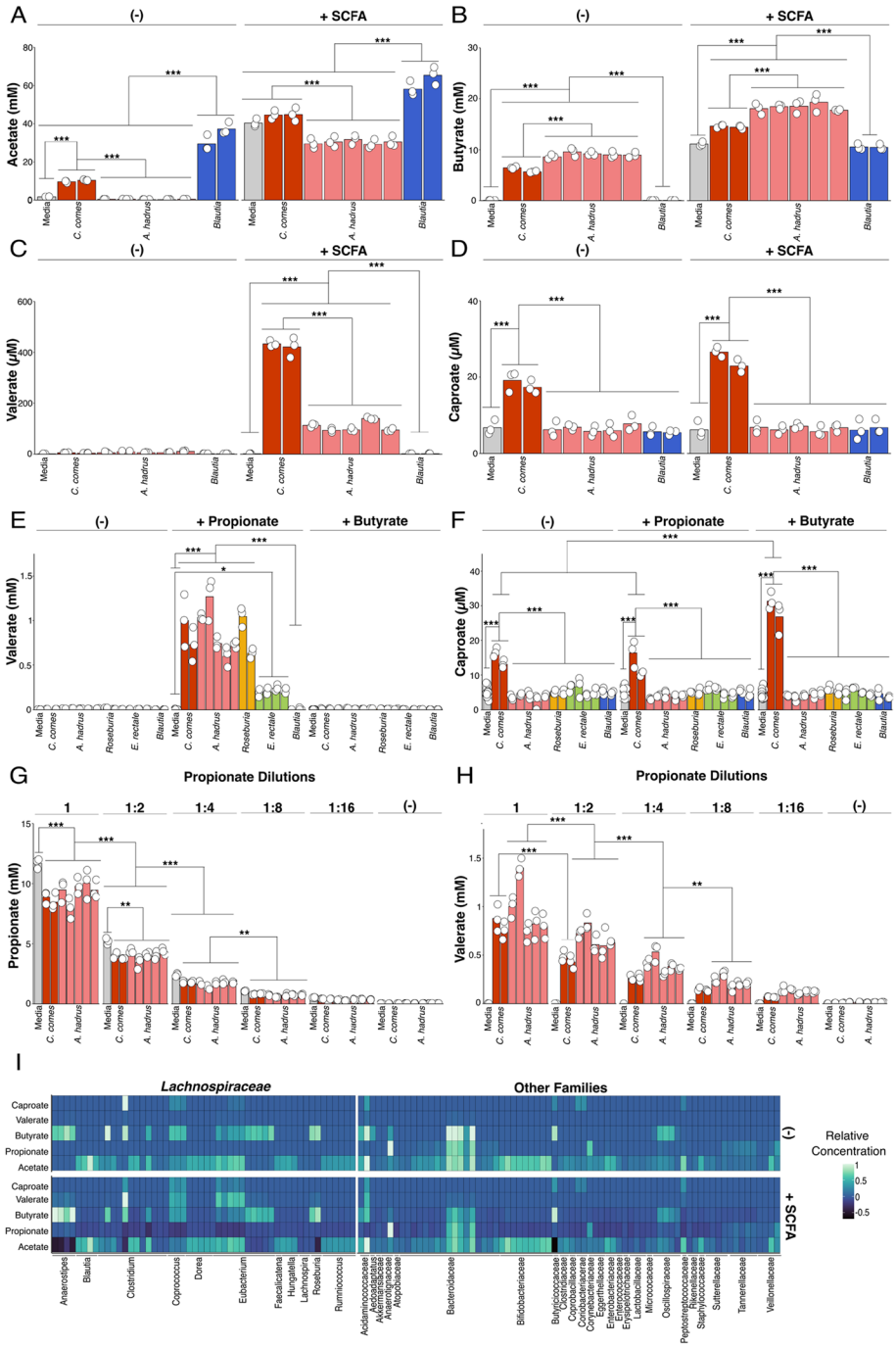

Fig. 2 SCFAs regulate production of valerate and caproate by *Lachnospiraceae*. **A**–**D** Production of **A** acetate, **B** butyrate, **C** valerate, and **D** caproate by 2 *C. comes*, 5 *A. hadrus*, and 2 *Blautia* strains with or without a physiological mixture of acetate, propionate, butyrate (+ SCFA). **E**, **F** Production of (**E**) valerate and (**F**) caproate by 2 *C. comes*, 5 *A. hadrus,* 2 *Roseburia*, 4 *E. rectale*, and 2 *Blautia* strains with supplementation of propionate or butyrate. **G**, **H** Production of valerate (**H**) with decreasing levels of **G** propionate by 2 *C. comes* and 5 *A. hadrus* strains. **I** Relative concentrations of SCFAs, valerate, and caproate by strains in the donor-derived community with and without SCFA supplementation. For **I**, values shown are the mean of 3 biological replicates. For **A–H**, bars show the mean value, and points show individual values of 3 biological replicates. Statistical tests were performed by one-way ANOVA with post-hoc Tukey test (* indicates $p < 0.05$, ** $p < 0.01$, *** $p < 0.001$)

valerate levels were higher compared to levels in mixed SCFA conditions, averaging 875 μM and 865 μM in *A. hadrus* and *C. comes* cultures respectively (Fig. 2CE, S2GH). Culture densities of *C. comes, E. rectale, Roseburia* spp., and *Blautia* spp. were not altered by propionate addition, while some strains of *A. hadrus* showed increased growth (Fig. S2F). Conversely, supplementation with butyrate, but not propionate, increased caproate production by *C. comes,* while no other isolates produced caproate (Fig. 2F). For most strains, butyrate supplementation did not alter culture density, while a single *E. rectale* strain showed decreased density (Fig S2F). Propionate-activated valerate production was dose dependent and varied with propionate levels across a physiological range of concentrations (Fig. 2G, H). In these experiments, extracellular propionate levels tended to decrease when valerate was produced (Fig. 2GH).

To investigate SCFA-activated valerate and caproate production more broadly, we grew strains present in the model gut community individually. Under control conditions, valerate production was low for all constituents but increased in a subset of butyrate-producing *Lachnospiraceae* with SCFA supplementation averaging 355 μM (Fig. 2I, Table S2). Furthermore, while a limited number of strains produced low levels of caproate at baseline, production was increased with SCFA supplementation in a subset of butyrate-producing *Lachnospiraceae*, including strains of *C. comes* (Fig. 2I). Further, we noted that within the *Bacteroidaceae* family, strains of *Bacteroides kribbi* also produced low levels of valerate, but not caproate (Fig. 2I, Table S2). Production of valerate by *B. kribbi* was lower than that by *Lachnospiraceae*, did not require SCFA supplementation, and remained < 75 μM across conditions. Distinct from valerate-producing *Lachnospiraceae,* the tested *B. kribbi* strains also produced isobutyrate/isovalerate and strongly depleted valine, isoleucine, leucine, and glutamate (Fig. S2B–D).

Direct incorporation of exogenous SCFAs into valerate and caproate by *Lachnospiraceae*

Next, we asked if *Lachnospiraceae* directly incorporate extracellular SCFAs into valerate and caproate by combining acetate with propionate to yield valerate, or acetate with butyrate to yield caproate. To address this, five strains of *A. hadrus* and two strains of *C. comes* were grown with ^{13}C isotopically labelled SCFAs. Inclusion of + 2 acetate in the physiological SCFA mixture led to production of + 2 butyrate by *A. hadrus* and *C. comes* (Fig. 3A and Fig. S3A). In addition, labelled acetate was incorporated into + 2 valerate by *C. comes* and *A. hadrus*, and + 2, + 4, + 6 caproate by *C. comes* (Fig. 3A and Fig. S3A). Strains of *C. comes*, which are net acetate producers, showed reduced incorporation of exogenous + 2 acetate into butyrate (9% + 2 butyrate) and valerate (17% + 2 valerate), compared to strains of *A. hadrus* (32% and 50%, respectively), which are net consumers of exogenous acetate (Figs. 2A and 3A). Strikingly, when + 3 propionate was provided, all valerate produced by *C. comes* or *A. hadrus* was detected as + 3 valerate, with no labelling of butyrate or caproate (Fig. 3B and Fig. S3B). Supplementation with + 4 butyrate resulted in production of + 4 caproate only in *C. comes* cultures (Fig. 3C and Fig. S3C). Finally, to directly test if exogenous acetate and propionate could be combined to produce valerate, we grew *Lachnospiraceae* with both + 2 acetate and + 3 propionate. This led to the production of both + 3 and + 5 valerate, consistent with a condensation reaction between exogenous propionate and either exogenous or endogenous acetate (Fig. 3D and Fig. S3D). Altogether, this shows that *Lachnospiraceae* directly incorporate exogenous SCFAs into valerate and caproate.

Activating valerate production by *Lachnospiraceae*

We next investigated if valerate production by *Lachnospiraceae* could be rationally modulated without the addition of exogenous SCFAs. In baseline conditions, tested strains of *C. comes* and *A. hadrus* produce butyrate but do not produce propionate (Fig. 2A and Fig. S2A). However, members of *Anaerostipes* produce propionate when grown on inositol in a strain-specific manner [53]. Therefore, we asked if providing inositol to trigger propionate production would result in subsequent valerate production. In agreement with earlier reports, we observed strain-specific propionate production by *A. hadrus* with inositol supplementation, while tested *C. comes* strains did not produce propionate (Fig. 4A). As predicted, this also increased valerate production in the inositol-metabolizing *A. hadrus* strains (Fig. 4B). In growth media without dextrose or inositol, *A. hadrus* strains produced low amounts of propionate and valerate. Interestingly, valerate production had slightly slower accumulation kinetics compared to propionate, consistent with the valerate production kinetics observed in community cultures (Fig. 4C, Fig. 1C).

We observed that *Anaerotignum lactatifermentans*, a member of the model microbiota, produces high levels of propionate (Fig. 2I). Therefore, we tested if co-culturing butyrate-producing *A. hadrus or C. comes* with *A. lactatifermentans* isolates would activate valerate production. In monocultures, *A. lactatifermentans* produces 11 mM of propionate but does not produce valerate (Fig. 4D). In contrast, co-cultures of *A. lactatifermentans* with *A. hadrus* and *C. comes* produce 92 and 175 μM of valerate respectively, indicative of propionate cross-feeding from *A. lactatifermentans* to *A. hadrus* and *C. comes* (Fig. 4E). Next, we asked if the addition of *A. lactatifermentans*

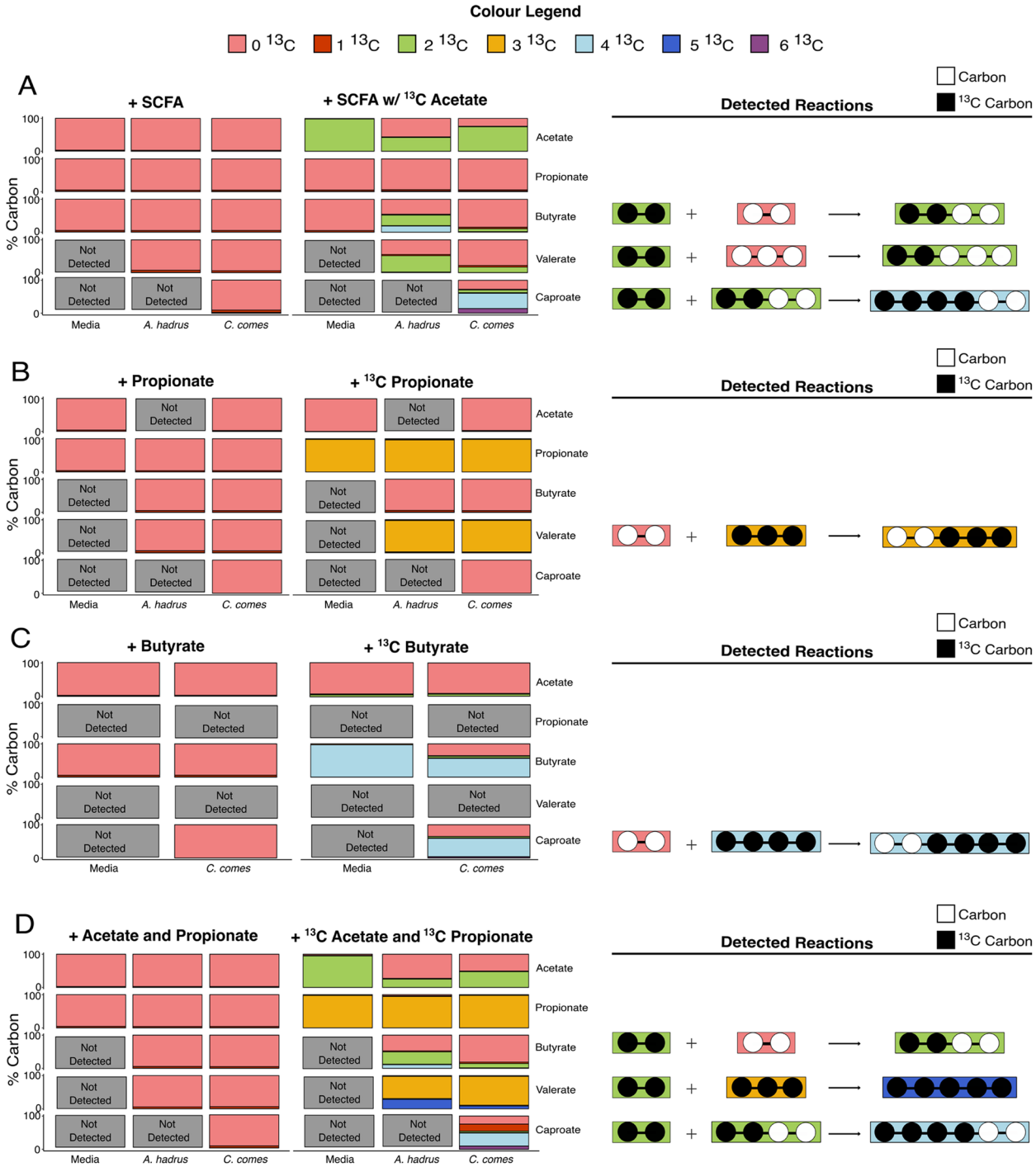

Fig. 3 *Lachnospiraceae* incorporate exogenous SCFAs into valerate and caproate. **A** Incorporation of $2^{13}C$ acetate into butyrate, valerate, and caproate by 5 *A. hadrus* and 2 *C. comes* strains. **B** Incorporation of $3^{13}C$ propionate into valerate by 5 *A. hadrus* and 2 *C. comes* strains. **C** Incorporation of $4^{13}C$ butyrate into caproate by 2 *C. comes* strains. **D** Incorporation of $2^{13}C$ acetate and $3^{13}C$ propionate into butyrate, valerate and caproate by 5 *A. hadrus* and 2 *C. comes strains*. Values shown in **A**–**D** are mean values of 3 biological replicates for 5 *A. hadrus* and 2 *C. comes* strains. Data for individual strains is presented in (Fig. S3). $1^{13}C$, $2^{13}C$, $3^{13}C$, $4^{13}C$, $5^{13}C$, and $6^{13}C$ masses of the SCFA, valerate and caproate are represented by the indicated colours. In detected reactions, schematics show normal carbons and ^{13}C carbons represented by white and black respectively

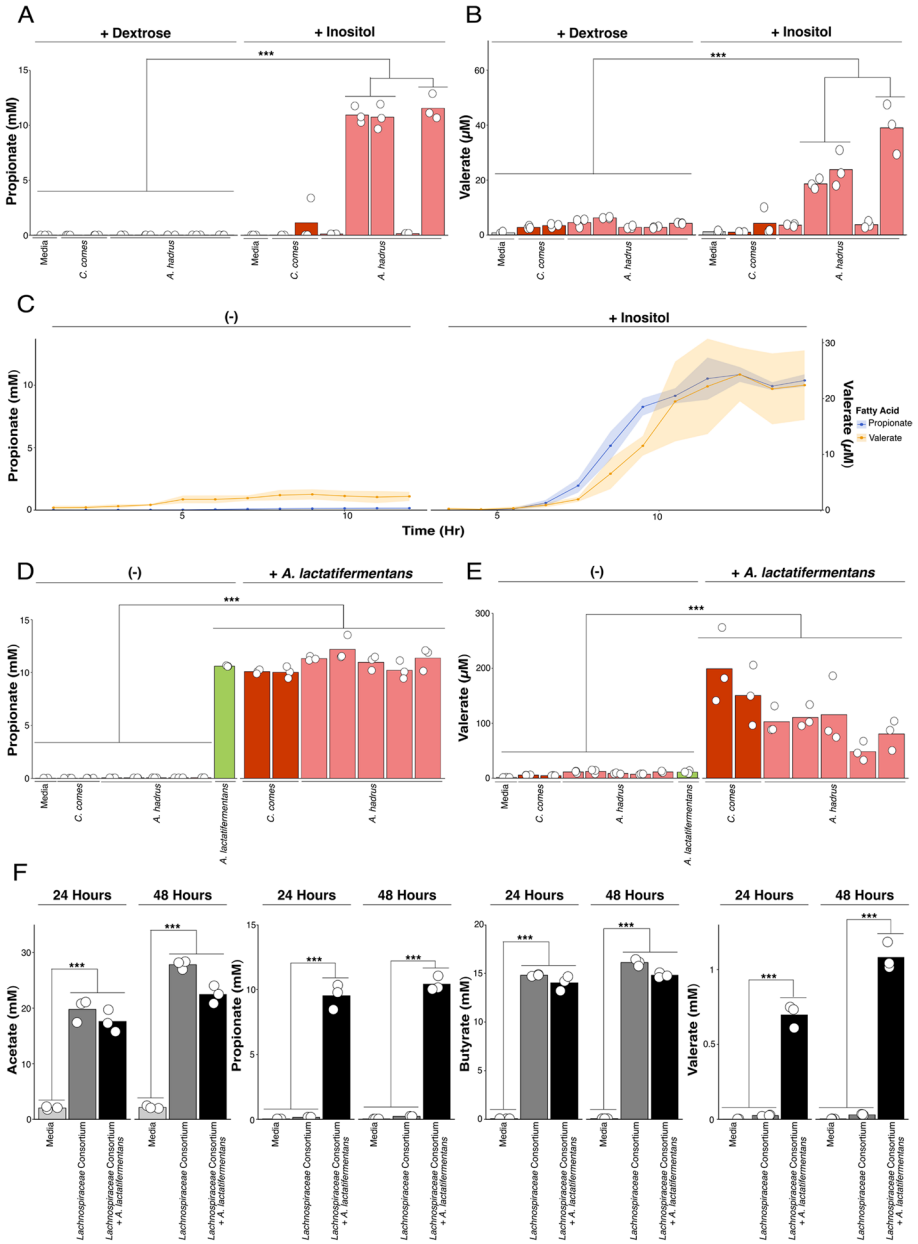

Fig. 4 Carbon source and co-culture conditions regulate valerate production in *Lachnospiraceae*. **A**, **B** Strain-dependent production of **A** propionate by 5 *A. hadrus* and 2 *C. comes* strains increases **B** valerate production during inositol supplementation. **C** Accumulation of propionate and valerate by inositol-utilizing *A. hadrus* with or without inositol supplementation (mean ± standard deviation of 3 biological replicates). **D**, **E** Production of propionate **D** by an *A. lactatifermentans* strain supports **E** valerate production in co-culture with *A. hadrus* and *C. comes* strains. **F** Production of acetate, propionate, butyrate, and valerate in co-cultures of *A. lactatifermentans* with a mixture of 6 *Lachnospiraceae* species (1 strain of *A. hadrus, C. comes, Blautia luti, Clostridium innocuum, Clostridium symbiosum*, and *Dorea longicatena*). For **A**, **B**, **D**, **E**, **F**, bars show the mean value, and points show individual biological replicates. Statistical tests were performed by one-way ANOVA with post-hoc Tukey test (* indicates $p < 0.05$, ** $p < 0.01$, *** $p < 0.001$)

to a consortium of six *Lachnospiraceae* would activate valerate production. Interestingly, this consortium produces both acetate and butyrate but not propionate or valerate at baseline. In contrast, co-cultures of the *Lachnospiraceae* consortium with *A. lactatifermentans* produce 22 mM of acetate, 10 mM of propionate, 15 mM of butyrate, and 1 mM of valerate (Fig. 4F). Overall, this demonstrates that growth conditions and model communities can be controlled to activate *Lachnospiraceae* valerate production.

Lachnospiraceae encode multiple variants of acetyl-CoA acetyltransferase proteins

Next, we examined the pathway of valerate production in *Lachnospiraceae*. The gut microbiota can ferment amino acids including valine, isoleucine, leucine, and glutamate to yield valerate, isobutyrate, and isovalerate [22, 23, 54]. However, valerate-producing *Lachnospiraceae* did not deplete these amino acids or produce isobutyrate/isovalerate (Fig. S2B, C). Alternatively, *Megasphaera* spp. produces butyrate, valerate, and caproate through a reverse β-oxidation pathway that depends on a ThlA enzyme (EC 2.3.1.9) (Fig. 5A) [10, 26]. ThlA performs a condensation reaction between two acyl-CoA molecules in a stepwise reaction catalyzed by conserved catalytic cysteine residues. Therefore, we performed comparative genomic analyses of the reverse β-oxidation pathway of *Lachnospiraceae* that functions in butyrate production (Fig. S4A.B) [8]. This revealed that, unlike other *Lachnospiraceae* isolates in our panel, *C. comes* strains, which produce both valerate and caproate, encode two copies of thlA, referred to here as thlA_1 and thlA_2. Similarly, *Megasphaera,* which also produces both valerate and caproate, encodes two thlA copies (Fig. S4B). Therefore, we sought to investigate the use of different acyl-CoA's by *Lachnospiraceae* ThlA enzymes in the first step of the reverse β-oxidation pathway.

First, we compared ThlA protein sequences across a collection of gut microbes [27, 40–42] which revealed extensive diversity, particularly within the *Lachnospiraceae* family (Fig. 5B). We noted that *C. comes* ThlA_1 clustered with ThlAs from other *Lachnospiraceae* species, whereas ThlA_2 was distinct and clustered with ThlAs from *Megasphaera* spp. (Fig. 5B). In agreement, ThlA_2 shared less than 70% sequence identity with other ThlA proteins from our tested panel of isolates, including ThlA_1 (Fig. 5C). Next, we examined the genomic context of *Lachnospiraceae* thlA genes. In tested *C. comes* isolates, *thlA_2* is adjacent to the gene cluster containing *thlA_1* and genes encoding the reverse β-oxidation pathway (Fig. 5D). Despite sequence variation, overall, the Alphafold 3 predicted structures of *C. comes* ThlA_1 and ThlA_2, and *A. hadrus* ThlA were similar, especially in the position of their catalytic cysteine residues (Fig. 5E).

Next, we asked if *Lachnospiraceae* ThlA variants could use acyl-CoA substrates consistent with the observed patterns of valerate and caproate production. To test this, we expressed *C. comes* ThlA_1, *A. hadrus* ThlA, and *C. comes* ThlA_2 in *E. coli* and purified the proteins. Using the purified proteins, ThlA assays were performed with different acyl-CoA substrates and an Hbd protein to favor the forward reaction [48]. ThlA activity was measured by observing the consumption of acyl-CoA substrates (Fig. S5A). In reactions with acetyl-CoA, all three enzymes depleted similar amounts of acetyl-CoA (Fig. 5F). To test if these ThlA variants could support valerate production, we performed assays with both acetyl- and propionyl-CoA. All three enzymes were able to deplete propionyl-CoA along with acetyl-CoA (Fig. 5F) consistent with the valerate production capabilities of both *C. comes* and *A. hadrus*. Given the restricted production of caproate, we hypothesized that the *C. comes* ThlA_2 protein might be the enzyme primarily responsible for condensing butyryl-CoA and acetyl-CoA in caproate biosynthesis. In agreement, when butyryl-CoA and acetyl-CoA were provided, ThlA_2 depleted significantly more butyryl-CoA compared to other tested variants (Fig. 5F). Therefore, the second copy of ThlA showed unusually high turnover of butyryl-CoA, consistent with the unique ability of *C. comes*, among these isolates, to produce caproate. Structural models of ThlA_2 show a significantly deeper substrate-binding tunnel than its homologs; in Chai-1 models, this tunnel is able to accommodate acetobutyryl-CoA in a catalytically competent conformation without significant van der Waals clashes (Fig. 5G).

Given the ability of all three tested ThlA proteins to utilize propionyl-CoA, we asked if strains of *A. hadrus* and *C. comes* convert extracellular propionate into intracellular propionyl-CoA. To investigate this, we quantified propionyl-CoA levels from whole-cell lysates of *A. hadrus* and *C. comes* following supplementation with ^{13}C isotopically labelled propionate. As expected, following + 3 propionate supplementation, both species produce + 3 propionyl-CoA, which indicates they convert exogenous propionate to intracellular propionyl-CoA (Fig. S5B).

Valerate and caproate production across members of the gut microbiota

Next, we investigated the distribution of thlA and reverse β-oxidation genes across 3766 gut microbiota isolates from published biobanks [27, 40–42]. ThlA genes are restricted to the *Bacillota* and *Pseudomonadota* phyla, with varying copy numbers (Fig. 6A). Further, isolates which encode two copies of *thlA* and a complete reverse β-oxidation pathway accounted for only 1.2% (44 isolates) of the total isolates, of which the majority belong to the *Lachnospiraceae* and *Clostridiaceae* families, along with *Megasphaera* isolates in *Veillonellaceae* (Fig. 6B), suggesting a specialist function in valerate and caproate production.

Next, we examined the presence of these genera in the Human Microbiome Project (HMP) dataset [32, 33]. First, we compared the abundance and prevalence of the tested *Lachnospiraceae* genera to *Megasphaera*. Across 440 healthy and 1198 IBD patient samples, tested genera of valerate-and caproate-producing *Lachnospiraceae*

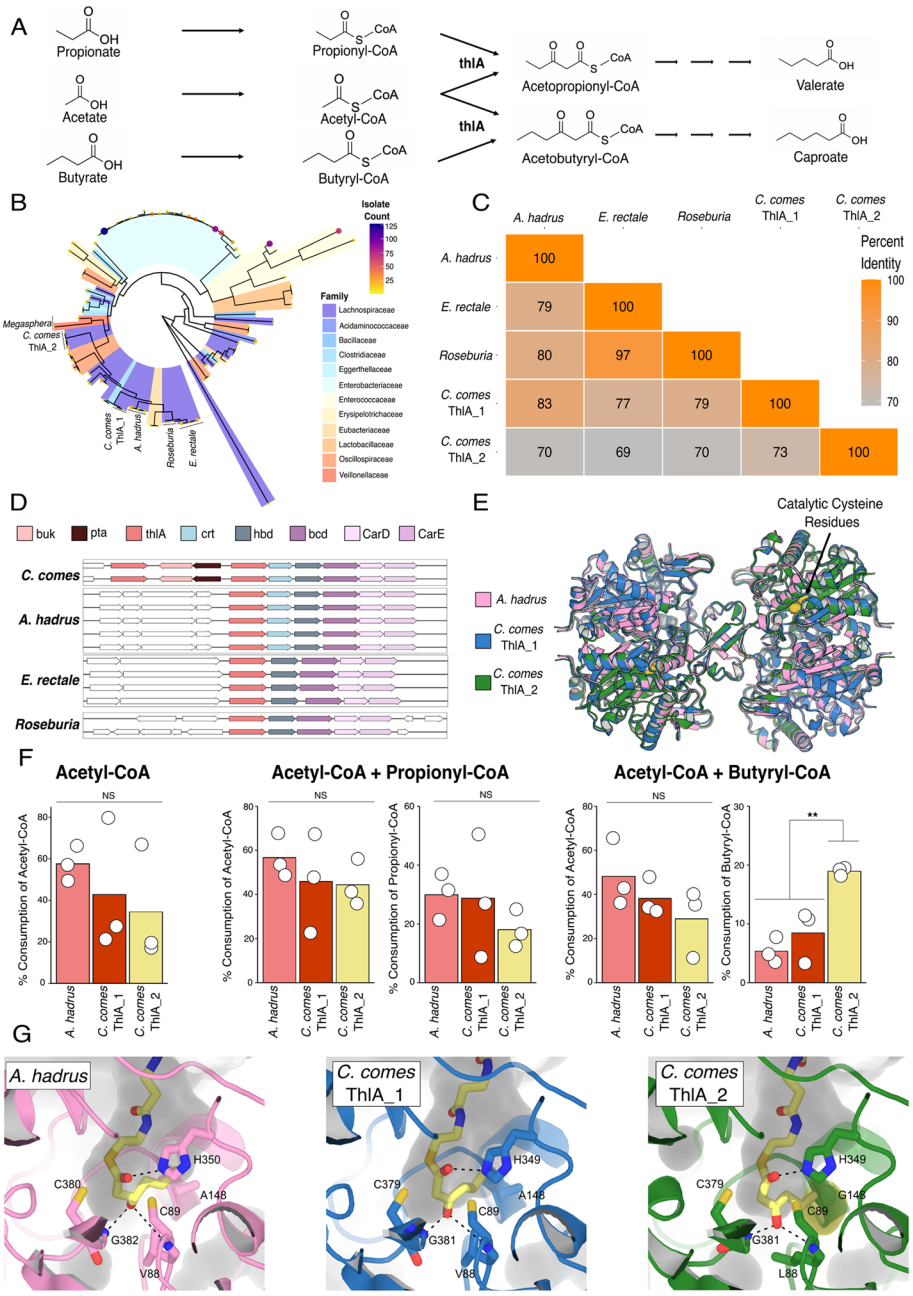

Fig. 5 *Lachnospiraceae* Acetyl-CoA acetyltransferase proteins vary in their ability to act on acyl-CoA metabolites. **A** Schematic showing production of valerate and caproate via a reverse β-oxidation pathway which is dependent on acetyl-CoA acetyltransferase (ThlA). **B** Maximum likelihood tree of ThlA proteins across gut microbes (tip size and colour represent number of isolates with identical sequences). **C** Percent identity of ThlA proteins from *A. hadrus*, *E. rectale, Roseburia, C. comes* (ThlA_1), and *C. comes* (ThlA_2). **D** Map of reverse β-oxidation gene cluster in *A. hadrus*, *E. rectale, Roseburia*, and *C. comes*. **E** Superimposed Alphafold predicted tetrameric structure of ThlA from *A. hadrus* and *C. comes* with catalytic cysteine residues represented in yellow. *A. hadrus*, *C. comes* (ThlA_1), and *C. comes* (ThlA_2) are represented by pink, blue and green, respectively. **F** Consumption of acetyl-CoA (left), acetyl-CoA and propionyl-CoA (middle), and acetyl-CoA and butyryl-CoA (right) by *A. hadrus*, *C. comes* (ThlA_1), and *C. comes* (ThlA_2) ThlA proteins. **G** Details of the active site of by *A. hadrus*, *C. comes* (ThlA_1), and *C. comes* (ThlA_2) ThlA proteins. Models of the acetobutyryl-CoA product complex were built in Chai-1. In each case, the substrate is positioned in a catalytically productive conformation, but only in *C. comes* (ThlA_2), is the active site tunnel deep enough to accommodate the longer substrate without steric clashes (highlighted in a yellow tint). Statistical tests were performed using a pairwise *t*-test with Bonferroni correction (* indicates $p < 0.05$, ** $p < 0.01$, *** $p < 0.001$)

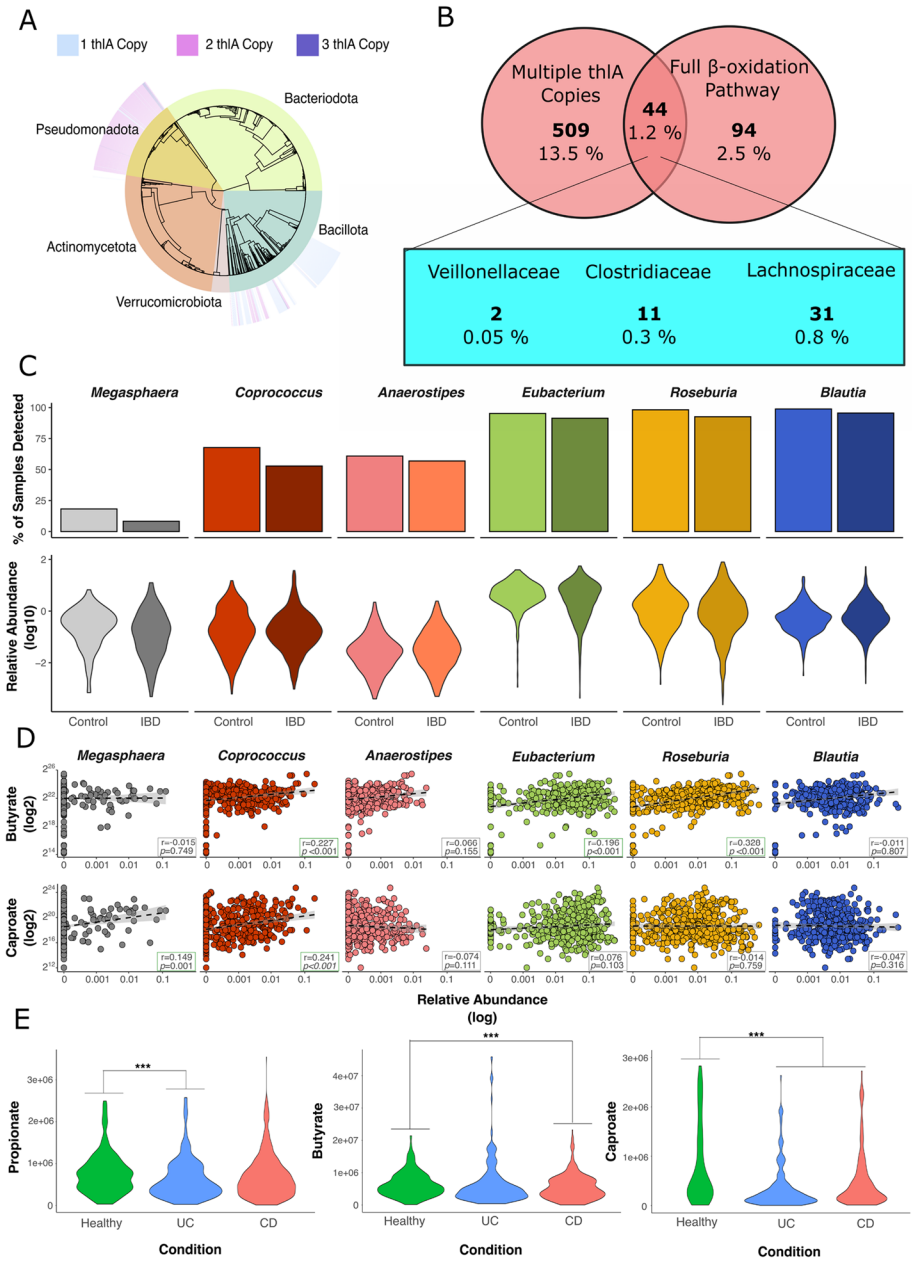

Fig. 6 *Lachnospiraceae* correlate with butyrate and caproate production in the human microbiota. **A** 16S rRNA dendrogram of gut microbes with the copy number of the encoded *thlAs*. 1, 2, and 3 represented by light blue, pink, and navy blue, respectively. **B** Overlap of the gut microbes which encode multiple *thlA* copies and the entire reverse β-oxidation pathway. **C** Prevalence of indicated genera in human fecal samples from the HMP project and their relative abundance. **D** Spearman correlation between abundance of indicated genera and butyrate and caproate levels. **F** Levels of propionate, butyrate, and caproate in healthy, ulcerative colitis (UC) and Crohn's disease (CD) patients. Statistical tests were performed by one-way ANOVA with post-hoc Tukey test (* indicates $p < 0.05$, ** $p < 0.01$, *** $p < 0.001$)

were more prevalent and abundant than *Megasphaera* (Fig. 6C). *Megasphaera* was detected in < 15% of samples at an average relative abundance of 6.7×10^{-4}. In contrast, *Coprococcus*, *Anaerostipes*, *Eubacterium*, and *Roseburia* were detected in 57%, 58%, 92%, and 94% of samples, respectively (Fig. 6C). Furthermore, these genera were detected at average relative abundances of 4.6×10^{-3}, 6.6×10^{-4}, 5.8×10^{-2}, and 3.5×10^{-2}, respectively (Fig. 6C). This suggests that for most microbiota community compositions, butyrate-producing *Lachnospiraceae* are a likely primary source of valerate and caproate production.

Next, we examined paired metabolomics data[32,33], and correlated butyrate and caproate levels with genera of *Lachnospiraceae* and *Megasphaera*. In this dataset, valerate was not distinguished from isovalerate. Except for *Anaerostipes*, the tested butyrate-producing *Lachnospiraceae* genera correlate with butyrate. Strikingly, only the *Coprococcus* and *Megasphaera* genera correlate with caproate, consistent with their ability to produce caproate (Fig. 6D). Finally, we compared levels of these metabolites between healthy controls and individuals with IBD (both Ulcerative Colitis (UC) and Crohn's disease (CD)). When compared to samples from healthy individuals, propionate levels are significantly lower in UC samples, while butyrate levels are significantly lower in CD samples. Interestingly, caproate was significantly lower in both UC and CD compared to the healthy samples (Fig. 6E).

Discussion

In this study, we found that extracellular SCFAs trigger valerate and caproate production by butyrate-producing *Lachnospiraceae* through the reverse β-oxidation pathway. Production of physiological levels of these important metabolites is species specific, with strains of *A. hadrus*, *E. rectale*, and *Roseburia* spp. producing valerate, whereas *C. comes* strains produce both valerate and caproate. These valerate- and butyrate-producing *Lachnospiraceae* are prevalent and abundant in the human microbiota (Fig. 6C) [32, 33]. Indeed, across tested *Lachnospiraceae* genera, several correlate with butyrate in human fecal samples, while only *C. comes* correlates with caproate (Fig. 6D). Therefore, in addition to their recognized role as important SCFA producers, select members of the *Lachnospiraceae* are also valerate and caproate producers.

The reverse β-oxidation pathway combines acyl-CoA molecules to create longer carbon chains [8, 29]. Previous studies have shown that this pathway is used by gut microbes, including *Lachnospiraceae*, to produce butyrate through the condensation of acetyl-CoA and acetyl-CoA [28]. We found that *Lachnospiraceae* use this pathway to combine acetate and propionate to produce valerate, with *C. comes* also being able to use acetate and butyrate to produce caproate. Indeed, *A. hadrus* and *C. comes* strains convert extracellular, isotopically labelled propionate into intracellular propionyl-CoA and directly incorporate exogenous SCFAs into valerate and caproate (Fig. 3, Fig. S3). However, while it is known that SCFAs are weak acids that become protonated and membrane permeable at acidic pH [11], the mechanisms and regulation of extracellular SCFA uptake that enable and account for use in valerate and caproate production remain to be fully characterized. Overall, through SCFA uptake, *Lachnospiraceae* employ the reverse β-oxidation pathway in a similar manner to *Megasphaera* [10, 26]. However, in contrast to *Megasphaera*, the tested valerate and caproate producing *Lachnospiraceae* are detected in most human gut microbiomes (Fig. 6) [32, 33].

Differences in endogenous SCFA production between *Lachnospiraceae* species can also influence patterns of valerate and caproate production. Under tested conditions, *C. comes* is a net acetate producer while *A. hadrus* is a net acetate consumer (Fig. 2). These findings are in line with previous literature examining acetate incorporation into butyrate by acetate producers and consumers [55]. As a result, *C. comes* uses endogenously produced acetate in place of exogenous 13C-acetate to a greater extent than *A. hadrus* (Fig. 3). *C. comes* can also use endogenously produced butyrate to produce caproate (Figs. 2 and 3). Similarly, with inositol supplementation, *A. hadrus* produces both endogenous propionate and valerate, albeit at lower levels compared to conditions with exogenous propionate supplementation. In line with previous work characterizing the pathway of inositol use in *Anaerostipes,* not all tested strains of *A. hadrus* in our assay were able to metabolize inositol and produce propionate [53].

Exogenous propionate incorporation into valerate occurs along with decreases in extracellular propionate levels (Fig. 2). Surprisingly, for some combinations of strains and SCFA conditions, the decrease in propionate is greater than the increase in released valerate (Fig. 2). While some of the consumed propionate will be cell-associated as propionyl-CoA (Fig. S5), or pathway intermediates/intracellular valerate, it is possible that propionate or propionyl-CoA could be used by *Lachnospiraceae* in additional ways that remain to be characterized. Along similar lines, we found that a mixture of SCFAs increases culture densities of valerate-producing *Lachnospiraceae* (Fig. S2). In agreement, growth enhancement with SCFA supplementation has been previously reported for *Lachnospiraceae* and other gut microbes [52, 56]. However, whether growth effects for these valerate-producing *Lachnospiraceae* strains are attributable to increased flux through reverse β-oxidation or other uses of SCFAs remains to be investigated.

The condensation reaction in the reverse β-oxidation pathway is performed by the ThlA enzyme (EC 2.3.1.9). For the pathway to produce valerate, *Lachnospiraceae* ThlA enzymes must act on a propionyl-CoA in place of one of the acetyl-CoA molecules. In agreement, propionyl-CoA is consumed in a mixture with acetyl-CoA by three *Lachnospiraceae* ThlA proteins (Fig. 5F) and valerate production increases with propionate supplementation (Fig. 2C, E, I). Interestingly, *C. comes* produced higher valerate when grown in the presence of a physiological SCFA mixture than other *Lachnospiraceae*, but

produced similar valerate levels as other species with sole-propionate supplementation (Fig. 2C, E, I). This indicates that there are species-specific responses to varying SCFA environments that remain to be explored.

C. comes encodes two thlA genes, and biochemical tests demonstrated greater consumption of butyryl-CoA with the ThlA_2 protein than either the ThlA_1 protein or the *A. hadrus* ThlA protein (Fig. 5F). Thus, the second ThlA enzyme likely contributes to the ability of *C. comes* to produce caproate. It is important to note that analyzing a wide range of ThlA proteins from gut microbes revealed substantial sequence variation in these proteins (Fig. 5B). The influence of this large-scale variation on ThlA protein function and differential substrate utilization, or potential differences in subsequent steps of the reverse β-oxidation pathway, remains to be fully explored.

B. kribbi strains produce valerate, isovalerate, and isobutyrate while depleting glutamate, valine, isoleucine, and leucine, which is consistent with amino acid fermentation, as previously reported (Fig. 2, S2) [24, 25]. Indeed, analyzed *Bacteroidaceae* genomes were not annotated to encode ThlA (Fig. 6). The existence of distinct pathways of valerate production in the microbiome raises the possibility that dietary alterations could impact the source and context of valerate and caproate production. On high-fiber diets that promote complex carbohydrate use by the microbiota and high levels of beneficial SCFA production, reverse β-oxidation may be the primary source of valerate and caproate. In contrast, high protein/low fiber diets that increase protein and amino acid use could increase amino acid-linked valerate production along with isovalerate/isobutyrate and other metabolites of protein use, which are often negatively associated with health [57, 58]. These potential changes in pathways of valerate production with diet remain to be explored.

Restoring valerate and caproate levels, which are decreased in IBD patients (Fig. 6) [18–21], by developing defined microbial consortia could represent a potential therapeutic approach. Our data indicates that including propionate-producing microbes or targeted carbon sources in *Lachnospiraceae*-containing consortia may support recovery of valerate in addition to the SCFAs acetate and butyrate. In agreement, inclusion of propionate-producing *A. lactatifermentans* in a consortium with six *Lachnospiraceae* strains yields both SCFAs and valerate, which reach physiological levels found in the human gut (Fig. 4) [4]. However, additional impacts of strain-strain interactions and nutrient competition on valerate and caproate production remain to be explored. Moreover, as these consortium experiments were performed in vitro, in vivo optimization of valerate and SCFA production or restoration has yet to be realized.

This study has demonstrated that selected *Lachnospiraceae* isolates produce physiological levels of valerate and caproate through their reverse β-oxidation pathway in response to SCFAs. Overall, this identifies an additional mechanism through which members of *Lachnospiraceae* can influence host health.

Supplementary Information

The online version contains supplementary material available at https://doi.org/10.1186/s40168-025-02220-9.

Supplementary Material 1: Figure S1. Reproducible development of the microbial community in a continuous culture model of the colon. Figure S2. *Lachnospiraceae* isolates produce SCFAs but not branched-chain SCFAs in the presence of exogenous SCFAs. Figure S3. Incorporation of exogenous SCFAs into valerate and caproate by individual isolates. Figure S4. *Lachnospiraceae* and *Megasphaera* encode reverse β-oxidation pathways. Figure S5. *Lachnospiraceae* convert exogenous propionate to propionyl-CoA.

Supplementary Material 2: Table S1. Bacterial strains.

Supplementary Material 3: Table S2. The raw values for Figures 1-6.

Supplementary Material 4: Table S3. The raw values for Figures S1-S5.

Acknowledgements
We would like to thank the Stephen Seah lab for providing us with the purified 17-β-hydroxysteroid dehydrogenase protein and Aimee Dawe for assistance with figure design.

Authors' contribution
B.G.F. performed experiments, performed GC-MS analysis, performed data analysis, prepared figures and performed statistical analyses. M.G. and M.S.K. performed ThlA protein structure analysis, expressed/purified all ThlA proteins and aided with activity assay. I.J.F. and S.J.V. ran continuous culture community experiments with guidance, protocols and equipment designed by E.A.V. L.H. performed inositol supplementation kinetic experiments and extracted DNA for whole-genome sequencing. J.F. performed *Lachnospiraceae* consortium experiments. M.T.S. and B.G.F. designed experiments, analyzed results, and co-wrote the manuscript. All authors have reviewed and edited the manuscript.

Funding
This work was supported by grants from the Canadian Institutes of Health Research (FRN 183725), Natural Sciences and Engineering Research Council (RGPIN-2024–04214), and the Weston Family Foundation (POP24-11464).

Data availability
Whole genome sequencing data is available in the NCBI Genome under BioProject PRJNA1231039. 16S rRNA sequencing data is available in NCBI Sequence Read Archive (SRA) under BioProject PRJNA1231039. All relevant data are present in the manuscript and supplementary information. The raw values for figures are provided in Tables S2 and S3.

Declarations

Ethics approval and consent to participate
Not applicable.

Consent for publication
Not applicable.

Competing interests
The authors declare no competing interests.

Received: 25 March 2025 Accepted: 4 August 2025
Published online: 01 October 2025

References

1. den Besten G, et al. The role of short-chain fatty acids in the interplay between diet, gut microbiota, and host energy metabolism. J Lipid Res. 2013;54:2325–40.
2. Oliphant K, Allen-Vercoe E. Macronutrient metabolism by the human gut microbiome: major fermentation by-products and their impact on host health. Microbiome. 2019;7:91.
3. Koh A, De Vadder F, Kovatcheva-Datchary P, Bäckhed F. From dietary fiber to host physiology: short-chain fatty acids as key bacterial metabolites. Cell. 2016;165:1332–45.
4. Høverstad T, Fausa O, Bjørneklett A, Bøhmer T. Short-chain fatty acids in the normal human feces. Scand J Gastroenterol. 1984;19:375–81.
5. Rey FE, et al. Dissecting the in vivo metabolic potential of two human gut acetogens. J Biol Chem. 2010;285:22082–90.
6. Trischler R, Roth J, Sorbara MT, Schlegel X, Müller V. A functional Wood-Ljungdahl pathway devoid of a formate dehydrogenase in the gut acetogens *Blautia wexlerae*, *Blautia luti* and beyond. Environ Microbiol. 2022;24:3111–23.
7. Reichardt N, et al. Phylogenetic distribution of three pathways for propionate production within the human gut microbiota. ISME J. 2014;8:1323–35.
8. Vital M, Howe AC, Tiedje JM. Revealing the bacterial butyrate synthesis pathways by analyzing (meta)genomic data. MBio. 2014. https://doi.org/10.1128/mbio.00889-14.
9. Rios-Covian D, et al. An overview on fecal branched short-chain fatty acids along human life and as related with body mass index: associated dietary and anthropometric factors. Front Microbiol. 2020;11:973.
10. Jeon BS, Choi O, Um Y, Sang B-I. Production of medium-chain carboxylic acids by *Megasphaera* sp. MH with supplemental electron acceptors. Biotechnol Biofuels. 2016;9: 129.
11. Sorbara MT, et al. Inhibiting antibiotic-resistant Enterobacteriaceae by microbiota-mediated intracellular acidification. J Exp Med. 2018;216:84–98.
12. Le Poul E, et al. Functional characterization of human receptors for short chain fatty acids and their role in polymorphonuclear cell activation. J Biol Chem. 2003;278:25481–9.
13. Yuille S, Reichardt N, Panda S, Dunbar H, Mulder IE. Human gut bacteria as potent class I histone deacetylase inhibitors *in vitro* through production of butyric acid and valeric acid. PLoS One. 2018;13: e0201073.
14. McDonald JAK, et al. Inhibiting growth of *clostridioides difficile* by restoring valerate, produced by the intestinal microbiota. Gastroenterology. 2018;155:1495-1507.e15.
15. Luu M, et al. Microbial short-chain fatty acids modulate CD8+ T cell responses and improve adoptive immunotherapy for cancer. Nat Commun. 2021;12:4077.
16. Luu M, et al. The short-chain fatty acid pentanoate suppresses autoimmunity by modulating the metabolic-epigenetic crosstalk in lymphocytes. Nat Commun. 2019;10:760.
17. Gao G, et al. Effects of valerate on intestinal barrier function in cultured Caco-2 epithelial cell monolayers. Mol Biol Rep. 2022;49:1817–25.
18. Liu M, et al. Revisiting the role of valeric acid in manipulating ulcerative colitis. Inflamm Bowel Dis. 2024;30:617–28.
19. Xu H-M, et al. Characterization of short-chain fatty acids in patients with ulcerative colitis: a meta-analysis. BMC Gastroenterol. 2022;22:117.
20. Zhuang X, et al. Systematic review and meta-analysis: short-chain fatty acid characterization in patients with inflammatory bowel disease. Inflamm Bowel Dis. 2019;25:1751–63.
21. De Preter V, et al. Faecal metabolite profiling identifies medium-chain fatty acids as discriminating compounds in IBD. Gut. 2015;64:447–58.
22. Friedrich CG, Mitrenga G. Utilization of aliphatic amides and formation of two different amidases by *Alcaligenes eutrophus*. Microbiology. 1981;125:367–74.
23. Chen PRS, Dauterman WC. Alkylamidase of sheep liver. Biochimica et Biophysica Acta (BBA) - Enzymology. 1971;250:216–23.
24. Van den Abbeele P, et al. The effect of amino acids on production of SCFA and bCFA by members of the porcine colonic microbiota. Microorganisms. 2022;10:762.
25. Buckel W. Unusual enzymes involved in five pathways of glutamate fermentation. Appl Microbiol Biotechnol. 2001;57:263–73.
26. Kim H, Jeon BS, Sang B-I. An efficient new process for the selective production of odd-chain carboxylic acids by simple carbon elongation using *Megasphaera hexanoica*. Sci Rep. 2019;9:11999.
27. Sorbara MT, et al. Functional and genomic variation between human-derived isolates of *Lachnospiraceae* reveals inter- and intra-species diversity. Cell Host Microbe. 2020;28:134-146.e4.
28. Vacca M, et al. The controversial role of human gut *Lachnospiraceae*. Microorganisms. 2020;8:573.
29. Louis P, Flint HJ. Diversity, metabolism and microbial ecology of butyrate-producing bacteria from the human large intestine. FEMS Microbiol Lett. 2009;294:1–8.
30. Henke MT, et al. Capsular polysaccharide correlates with immune response to the human gut microbe *Ruminococcus gnavus*. Proc Natl Acad Sci U S A. 2021;118: e2007595118.
31. Zaplana T, Miele S, Tolonen AC. *Lachnospiraceae* are emerging industrial biocatalysts and biotherapeutics. Front Bioeng Biotechnol. 2024;11: 1324396.
32. Proctor LM, et al. The integrative human microbiome project. Nature. 2019;569:641–8.
33. Lloyd-Price J, et al. Multi-omics of the gut microbial ecosystem in inflammatory bowel diseases. Nature. 2019;569:655–62.
34. Gianetto-Hill CM, et al. The robogut: a bioreactor model of the human colon for evaluation of gut microbial community ecology and function. Curr Protoc. 2023;3: e737.
35. Petrof EO, et al. Stool substitute transplant therapy for the eradication of Clostridium difficile infection: 'RePOOPulating' the gut. Microbiome. 2013;1:3.
36. McDonald JAK, et al. Evaluation of microbial community reproducibility, stability and composition in a human distal gut chemostat model. J Microbiol Methods. 2013;95:167–74.
37. Callahan BJ, et al. DADA2: High-resolution sample inference from Illumina amplicon data. Nat Methods. 2016;13:581–3.
38. Becattini S, et al. Rapid transcriptional and metabolic adaptation of intestinal microbes to host immune activation. Cell Host Microbe. 2021;29:378-393.e5.
39. Tamvakopoulos CS, Anderson VE. Detection of acyl-coenzyme a thioester intermediates of fatty acid β-oxidation as the *N*-acylglycines by negative-ion chemical ionization gas chromatography—mass spectrometry. Anal Biochem. 1992;200:381–7.
40. Poyet M, et al. A library of human gut bacterial isolates paired with longitudinal multiomics data enables mechanistic microbiome research. Nat Med. 2019;25:1442–52.
41. Zou Y, et al. 1,520 reference genomes from cultivated human gut bacteria enable functional microbiome analyses. Nat Biotechnol. 2019;37:179–85.
42. Bisanz JE, et al. A genomic toolkit for the mechanistic dissection of intractable human gut bacteria. Cell Host Microbe. 2020;27:1001-1013.e9.
43. Seemann T. Prokka: rapid prokaryotic genome annotation. Bioinformatics. 2014;30:2068–9.
44. Edgar RC. MUSCLE: a multiple sequence alignment method with reduced time and space complexity. BMC Bioinformatics. 2004;5:113.
45. Stamatakis A. RAxML version 8: a tool for phylogenetic analysis and post-analysis of large phylogenies. Bioinformatics. 2014;30:1312–3.
46. Abramson J, et al. Accurate structure prediction of biomolecular interactions with AlphaFold 3. Nature. 2024;630:493–500.
47. Chai Discovery. *et al.* Chai-1: Decoding the molecular interactions of life. *bioRxiv* Preprint at https://doi.org/10.1101/2024.10.10.615955 (2024).
48. Meriläinen G, Poikela V, Kursula P, Wierenga RK. The thiolase reaction mechanism: the importance of Asn316 and His348 for stabilizing the enolate intermediate of the Claisen Condensation. Biochemistry. 2009;48:11011–25.
49. Cummings JH, Pomare EW, Branch WJ, Naylor CP, Macfarlane GT. Short chain fatty acids in human large intestine, portal, hepatic and venous blood. Gut. 1987;28:1221–7.
50. Macfarlane Gt, Gibson Gr, Cummings Jh. Comparison of fermentation reactions in different regions of the human colon. J Appl Bacteriol. 1992;72:57–64.

51. den Besten G, et al. Gut-derived short-chain fatty acids are vividly assimilated into host carbohydrates and lipids. Am J Physiol Gastrointest Liver Physiol. 2013;305:G900–10.
52. Duncan SH, Barcenilla A, Stewart CS, Pryde SE, Flint HJ. Acetate utilization and butyryl coenzyme A (CoA):acetate-CoA transferase in butyrate-producing bacteria from the human large intestine. Appl Environ Microbiol. 2002;68:5186–90.
53. Bui TPN, et al. Conversion of dietary inositol into propionate and acetate by commensal *Anaerostipes* associates with host health. Nat Commun. 2021;12:4798.
54. Batstone DJ, Pind PF, Angelidaki I. Kinetics of thermophilic, anaerobic oxidation of straight and branched chain butyrate and valerate. Biotechnol Bioeng. 2003;84:195–204.
55. Duncan SH, et al. Contribution of acetate to butyrate formation by human faecal bacteria. Br J Nutr. 2004;91:915–23.
56. Peterson CT, et al. Short-chain fatty acids modulate healthy gut microbiota composition and functional potential. Curr Microbiol. 2022;79:128.
57. Portune KJ, et al. Gut microbiota role in dietary protein metabolism and health-related outcomes: the two sides of the coin. Trends Food Sci Technol. 2016;57:213–32.
58. Yao CK, Muir JG, Gibson PR. Review article: insights into colonic protein fermentation, its modulation and potential health implications. Aliment Pharmacol Ther. 2016;43:181–96.

Publisher's Note